The influence of the addition of rubber waste on the properties of polyurethane coatings subjected to aging processes

coatings

MDPI

Article

The Influence of the Addition of Rubber Waste on the Properties of Polyurethane Coatings Subjected to Aging Processes

Paulina Mayer-Trzaskowska [1,*], Monica Ferraris [2], Sergio Perero [2] and Mariola Robakowska [3,*]

[1] Faculty of Mechanical Engineering, Department of Lightweight Element Engineering, Foundry, and Automation, Wroclaw University of Science and Technology, Wyspiańskiego 27, 50-370 Wroclaw, Poland
[2] Applied Science and Technology Department, Politecnico di Torino, C.so Duca Degli Abruzzi 24, I-10129 Torino, Italy; monica.ferraris@polito.it (M.F.); sergio.perero@polito.it (S.P.)
[3] Institute of Chemical Technology and Engineering, Faculty of Chemical Technology, Poznan University of Technology, Berdychowo 4, 60-965 Poznan, Poland
* Correspondence: paulina.mayer-trzaskowska@pwr.edu.pl (P.M.-T.); mariola.robakowska@put.poznan.pl (M.R.)

Abstract: The influence of aging and thermal shock processes on polymer coating reinforced with various rubber fillers on an aluminum substrate was investigated. The coatings were made from a polyurethane matrix and two different reinforcement materials: EPDM and SBR rubber waste fillers. The samples were subjected to 100 thermal shock cycles. Each cycle lasted 1 h, comprising 30 min at 100 °C followed by 30 min at 40 °C. The aging tests were conducted in a SUNTEST XLS+ aging chamber from Atlas Material Testing Technology GmbH, in accordance with the applicable ISO 4892-1:2016 standard. Thermal shocks increased the impact resistance of coatings with EPDM and SBR fillers. Neither UV aging nor thermal shocks affected the impact or abrasion resistance of unfilled polyurethane coatings. FTIR analysis revealed that UV exposure significantly accelerates chemical degradation of PUR, though fillers—especially EPDM—enhanced stability by mitigating this effect. Thermal shocks induced surface-level changes, including the formation of oxygenated groups and the rearrangement of hydrogen bonds. Rubber waste fillers influenced surface and thermal properties, with EPDM maintaining better hydrophobicity and oxidation resistance, while SBR-filled coatings demonstrated higher thermal stability but greater flexibility and susceptibility to degradation after aging.

Keywords: polyurethane coating; waste rubber fillers; impact and abrasion resistance; aging process; thermal properties; FTIR

Academic Editors: Yu Liu, Yali Gao, Dongdong Zhang and Bingbing Wang

Received: 29 April 2025
Revised: 27 May 2025
Accepted: 1 June 2025
Published: 3 June 2025

Citation: Mayer-Trzaskowska, P.; Ferraris, M.; Perero, S.; Robakowska, M. The Influence of the Addition of Rubber Waste on the Properties of Polyurethane Coatings Subjected to Aging Processes. *Coatings* **2025**, *15*, 677. https://doi.org/10.3390/coatings15060677

1. Introduction

One of the most effective and scientifically sound methodologies for the recycling of elastomeric residues, which are byproducts of various industrial processes, involves the strategic incorporation of these materials into composite materials that can serve multiple functional purposes. The examination and analysis of these newly formulated coatings hold significant relevance with regard to the reduction of overall costs associated with production, the minimization of raw material consumption, as well as the attenuation of

new waste generation, all of which contribute to the broader goals of sustainable development and environmental preservation.

Rubber waste fillers, derived from recycled materials such as waste tires, are used in applications like asphalt, playground surfaces, and sports fields, providing durability while reducing waste [1–4]. Additionally, rubber powder, produced from grinding waste rubber, serves as an effective filler in plastics and adhesives, improving mechanical properties and promoting eco-friendliness [5]. Rubberized asphalt, made with crumb rubber, improves road elastic recovery and resistance to cracking. Composite materials with rubber waste fillers are strong and flexible, making them suitable for automotive and construction applications. Rubber filler integrates recycled materials into rubber compounds, supporting sustainable production practices. These innovations underscore the versatility and environmental benefits of rubber waste fillers.

Polyurethane coatings are characterized by excellent resistance to abrasion, corrosion, chemicals, and changing weather conditions. Polyurethane coatings have many advantages, including durability, versatility, and resistance to various factors [6]. They are known for their high resistance to moisture, scratches, and chemicals. Polyurethane coatings also provide excellent adhesion, can be applied to various surfaces, and offer seamless insulation [7,8]. The polyurethane coatings used are flexible materials, which allows them to dissipate impact energy. This flexibility helps them maintain mechanical properties even after long-term use. Polyurethanes are designed to resist degradation when exposed to external factors such as UV radiation, moisture, and temperature. This allows them to maintain their properties for longer periods of time. Polyurethanes tolerate temperature changes well, allowing them to adapt to thermal shocks. Their structure allows for stress dissipation, which minimizes the risk of cracking [9].

Due to the opportunity of modifying their chemical structure, it is possible to adapt the properties of coatings to specific applications. Flexible polyurethanes find extensive application across a multitude of industries, encompassing sectors such as furniture manufacturing, medical devices, wood substitutes, electronics, packaging, construction, marine, and automotive engineering [10,11].

It is imperative to recognize that protective coatings, when exposed to various environmental conditions, are not immune to the effects of aging, which can significantly impact their performance over time. Depending on the type of climatic factor, polymer degradation can be categorized into several types, including oxidative and photo-oxidative degradation, thermal and thermo-oxidative degradation, ozone-induced degradation, as well as mechanical, chemical, and hydrolytic degradation [12–14]. The influence of climatic factors, including the ultraviolet (UV) radiation emitted from sunlight, as well as fluctuations in humidity and temperature, can instigate a plethora of chemical transformations within the coating material, potentially leading to adverse outcomes such as noticeable colour alterations, commonly referred to as yellowing, a decline in mechanical properties that are vital for structural integrity, or a deterioration in the adhesion quality between the coating and the underlying base material [12,14,15]. In practical applications, polymers are often exposed to multiple environmental stressors simultaneously, which may exert synergistic effects on material degradation. The concurrent influence of ultraviolet radiation and temperature fluctuations can markedly enhance the rate of polymer degradation [16]. Polymer aging tests in the natural environment take many years, which is why researchers rely mainly on accelerated aging tests [13,14,17–20].

Accelerated aging tests allow for the assessment of long-term durability of materials in days or weeks instead of years. This allows researchers to predict the behavior of coatings with different fillers or chemical modifications more quickly. Accelerated aging allows for the detection of degradation mechanisms (e.g., cracking, discoloration, flaking)

before they occur in reality, which helps in the design of more resistant materials. When introducing a new product to the market, it must comply with numerous standards and undergo a certification process. Conducting tests in advance helps to significantly reduce the time and cost involved [21,22].

The aim of this paper is to promote new solutions for the management of rubber waste and the production of polyurethane coatings with improved mechanical properties. The increasing accumulation of rubber waste highlights the need for its efficient management, aiming to minimize environmental impact and reduce the reliance on primary raw materials through cost-effective recovery and reuse strategies. The use of waste-derived fillers will reduce the amount of waste and have a positive impact on the environment. As environmental awareness grows and regulations become more stringent, the need for innovative solutions to recycle materials becomes more urgent. Developments in the rubber industry to find new, cost-effective uses for rubber waste are contributing to more sustainable waste management [23]. The use of rubber waste fillers in coatings has many benefits, such as reducing rubber waste, improving the physical properties of coatings, reducing production costs, and the possibility of creating more innovative and functional materials. From an environmental perspective, it is also a step towards more sustainable development that contributes to environmental protection [5].

The study is among the first to systematically investigate the combined effects of UV ageing and thermal shock on both mechanical and surface properties (impact resistance, abrasion resistance, hydrophobicity, and thermal stability) of PU coatings modified with different types of rubber fillers.

Prior research has explored rubber-modified polyurethane mainly in bulk elastomers or foams, with limited focus on thin-film coating systems. Moreover, those studies typically investigate single ageing conditions (e.g., only UV or thermal ageing), without evaluating combined stressors or dynamic performance shifts (e.g., microcracking). For example, works [24,25] investigated UV stability in SBR-based elastomers, but did not report on coating performance metrics like abrasion resistance, contact angle, or changes in T_g under combined ageing conditions.

The conducted research has practical and cognitive significance. Research on polyurethane coatings with rubber fillers has industrial potential. The conditions of mechanical properties research and ageing processes were selected in such a way as to obtain specific information on commercial polyurethane coatings with waste filler. After analyzing the existing literature, no similar research was found on the coatings described in the work. The research results show that the coatings can be successfully used in the industry.

2. Materials and Methods

2.1. Materials

As the substrate, the 1.0 mm thick PA11 aluminum sheet was chosen. Aluminum alloy PA11 is characterized by high corrosion resistance and fatigue strength. PA11 aluminum alloy is widely used in marine construction and construction of tanks, pipelines, or pneumatic lines due to its good weldability.

As a coating, Desmopol, Tecnopol Company, was chosen. It is a single-component liquid made up of polyurethane, and it is solvent-based and moisture-cured. Once catalyzed, it forms a continuous, seamless, watertight, and waterproof membrane. Polyurethanes are formed by a chemical reaction between a di/poly isocyanate (R-N=C=O) and a di/polyol (R′-OH), forming repeating urethane groups (R-NH-CO-R′). The coating is characterized by a tensile strength of 2 to 3 MPa and an elongation at break of ±600%. Its properties make it an excellent choice to be applied on a multitude of substrates of new buildings and especially in refurbishments.

As fillers, SBR (styrene-butadiene rubber) and EPDM (ethylene propylene diene monomer) rubber waste were used (Figure 1). The recovered SBR material consists of rubber elements from the household appliances industry (appliance seals) and from the industrial sector (conveyor belts, so-called rubber screeds from vulcanizing presses).

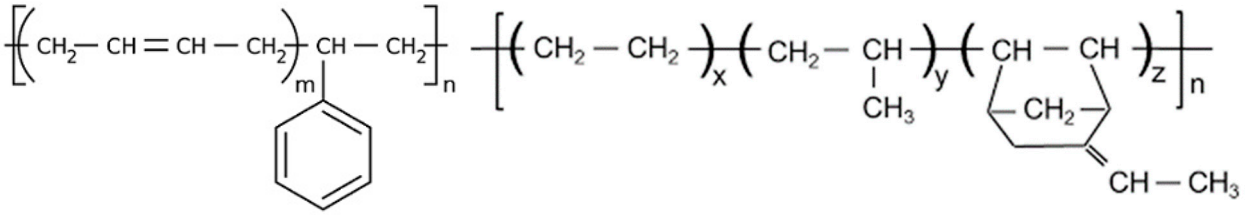

(**a**) (**b**)

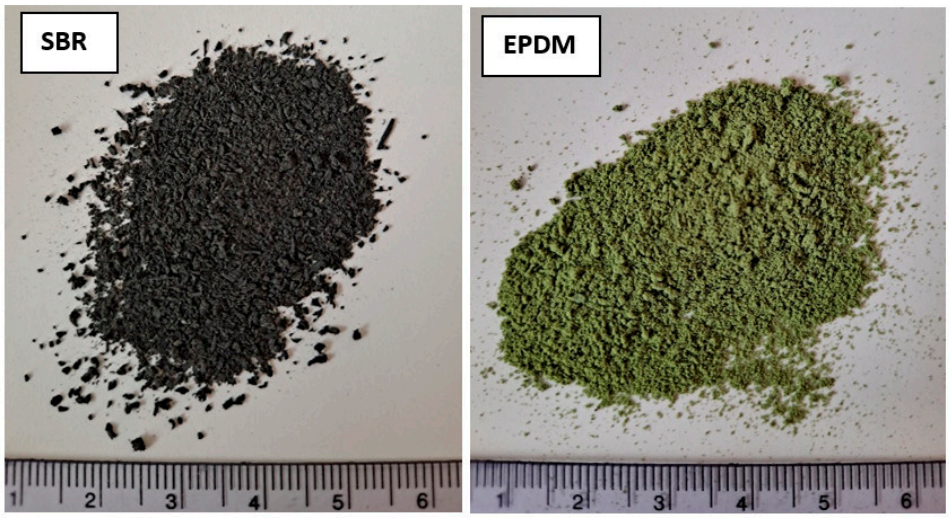

(**c**)

Figure 1. Chemical structure: (**a**) SBR (m = butadiene; n = styrene); (**b**) EPDM (x = ethylene, y = propylene, z = diene; (**c**) photos of waste rubber fillers.

Table 1 shows the samples obtained and their determination.

Table 1. Obtained coatings and their determination.

No.	Determination	Type of Filler	Type of Aging Process
1	**D_W**	-	without
2	**SBR_W**	SBR	without
3	**EPDM_W**	EPDM	without
4	**D_A**	-	UV aging
5	**SBR_A**	SBR	UV aging
6	**EPDM_A**	EPDM	UV aging
7	**D_TS**	-	thermal shock
8	**SBR_TS**	SBR	thermal shock
9	**EPDM_TS**	EPDM	thermal shock

The thickness of the resulting coatings was measured according to [26] standard using the magnetic method. Measurements were conducted with the MiniTest 730 FH5 device by ElektroPhysik™, which utilizes magnetic induction and eddy current techniques. Thickness of the obtained coatings is shown in Figure 2, and SEM cross-sections of the samples are shown in Figure 3.

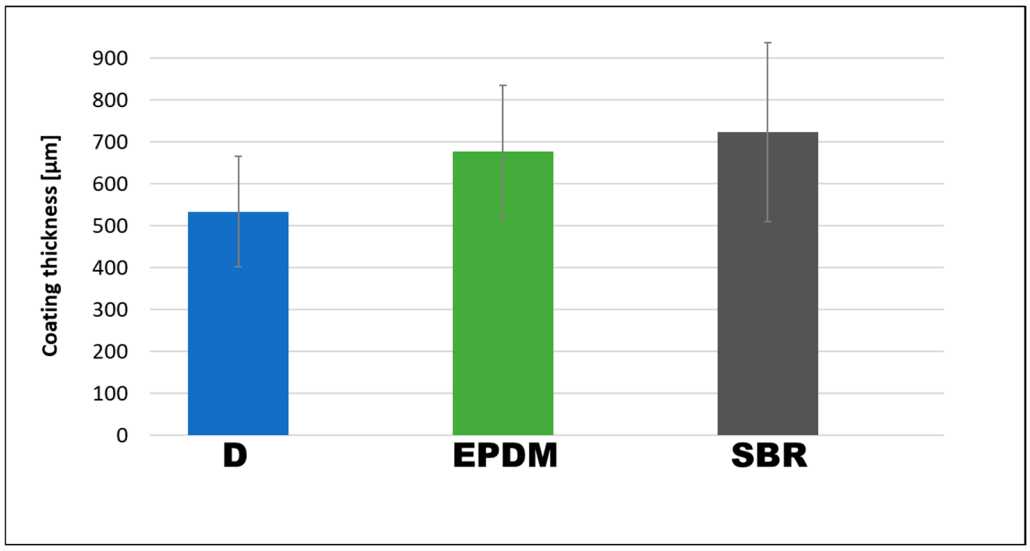

Figure 2. Thickness of the obtained coatings; D—sample without filler; SBR—sample with SBR filler; EPDM—sample with EPDM filler.

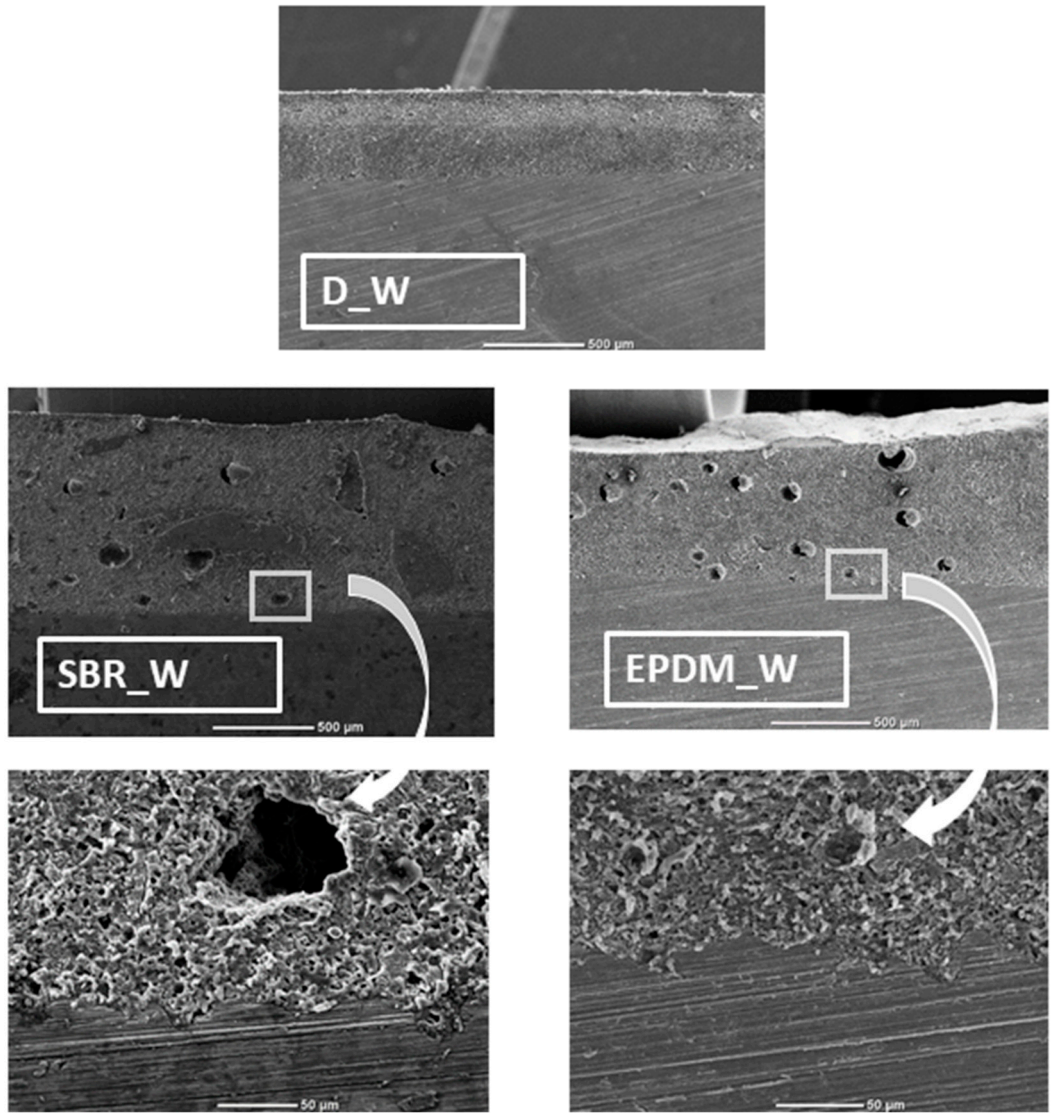

Figure 3. SEM cross-sections of samples.

The images (Figure 3) reveal significant differences in morphology and phase interaction depending on the type of elastomer introduced. The reference sample (D_W) exhibits a homogeneous and compact structure, with no visible defects such as voids, inclusions, or interfacial separations. This indicates high material integrity and confirms the proper execution of the synthesis. The incorporation of SBR (SBR_W) significantly affected the morphology of the polyurethane matrix. The dispersed domains are irregularly shaped, angular, and evenly distributed. Numerous voids and structural defects, including large, irregularly shaped pores, were observed. Adhesion between the filler and the polymer matrix is very important, as it significantly affects the mechanical properties [27,28]. The coating containing recycled EPDM (EPDM_W) showed a less porosity compared to the SBR-modified sample. A more uniform distribution of smaller, spherical pores was observed, indicating better dispersion of the elastomeric phase. Nevertheless, the presence of pores points to incomplete compatibility with the polyurethane matrix.

2.2. Methods

2.2.1. Aging Tests

The aging tests were conducted in a SUNTEST XLS+ aging chamber from Atlas Material Testing Technology GmbH, in accordance with the applicable [29]. Device monitors light in the range of 300–800 nm, so the dose was recalculated for the 295 nm–800 nm range for indoor light, which is 455 W/m^2. The aging process parameters were set according to these calculations, resulting in a radiation dose equivalent to a 1-month period of 169.8 MJ/m^2, corresponding to a device operating time of 104.3 h at a temperature of 65 °C.

2.2.2. Thermal Shock Process

A total of 100 thermal shock cycles were performed. Each cycle lasted 1 h: 30 min at 100 °C and 30 min at −40 °C. The temperature transition (100 °C to −40 °C) occurred within 4 s. Tests were conducted using a Heraeus/Vötsch chamber, model HT 7012 S2™.

2.2.3. Impact Resistance

Impact-resistance testing was conducted in accordance with the EN ISO 6272-1:2011 standard [30]. The tests employed a TQC SP1880-134 device (Figure 4a).

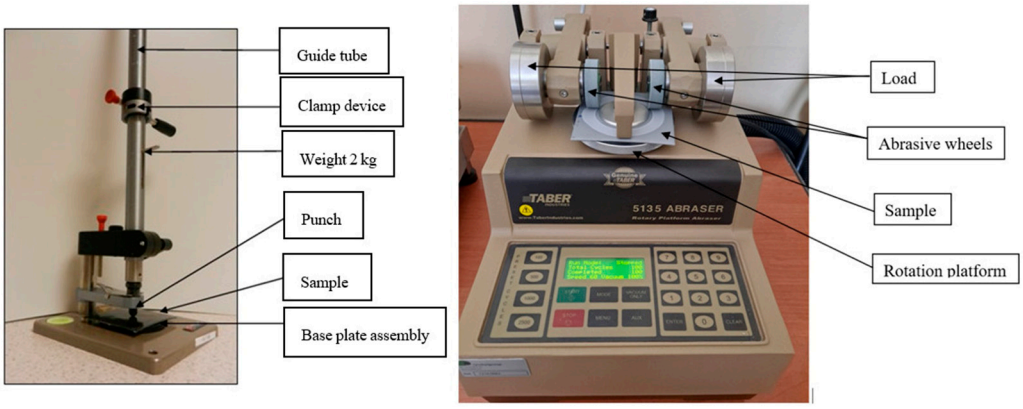

(**a**) (**b**)

Figure 4. Devices used in the tests; (**a**) impact resistance tester; (**b**) Taber Abraser.

The core component of the apparatus is a 2 kg weight with a hemispherical indenter tip measuring 20 mm in diameter, which is positioned at a specific height within a vertical

guide tube. The guide tube allows the weight to be released from a maximum height of 1000 mm. This method is used to determine the minimum drop height at which the coating sustains damage.

2.2.4. Abrasion Resistance Tests

The most common test method for the determination of abrasion resistance is the Taber Abraser method. The sample is mounted on a table rotating around a vertical axis and is subjected to abrasion by two wheels covered with abrasive material. The wheels are pressed against the sample by weights (Figure 4b).

It consists of measuring the weight loss occurring when the coated substrate is subjected to rotating abrasive wheels with a defined load.
Process parameters:

- platform rotation speed: 60 rpm;
- load on the abrasive wheel arms: 1000 g;
- abrasive wheels used: Calibrase H 18;
- abrasive paper for renewing the surface of abrasive wheels: S-11.

The sample underwent abrasion-resistance testing according to ASTM D-4060 standard [31]. Following the test, the samples were humid-cured for 24 h at 23 °C and 50% relative humidity, in accordance with ASTM D-4060. The worn surfaces were analysed using a stereoscopic microscope to investigate the material removal of the coating.

Taber Wear Index—indicates rate of wear, and is calculated by measuring the loss in weight (in mg) per number of cycles of abrasion. The lower the wear index, the better the abrasion resistance (1).

$$I = [(A - B) \times 1000]/C \quad (1)$$

where I = wear index, A = weight (mass) of specimen before abrasion, B = weight (mass) of specimen after abrasion, C = number of test cycles.

2.2.5. Thermal Properties

Thermal resistance was assessed using a TG 209 F3 Tarsus™ thermogravimetric analyzer (Netzsch-Gerätebau GmbH, Germany). Approximately 10 mg of each sample was placed in Al_2O_3 crucibles and heated from 40 °C to 650 °C at a rate of 10 °C/min in a nitrogen atmosphere, with a purge flow of 20 mL/min for protective gas and 30 mL/min for the sample gas. The decomposition temperatures corresponding to 10%, 50%, and 90% mass loss were recorded. The remaining mass (residue) was determined at approximately 600 °C. The glass transition temperature (T_g) was determined using a DSC1 differential scanning calorimeter (Mettler Toledo, Ohio, USA) under a nitrogen atmosphere. The heating rate was set to 20 °C/min. T_g values were obtained from the second heating cycle, conducted over the temperature range of 0 °C to 120 °C, with a 3-min isothermal hold at 0 °C before the scan.

2.2.6. FTIR Spectroscopy

Fourier-transform infrared (FTIR) spectra of the samples were recorded using attenuated total reflectance (ATR) mode. Measurements were performed with a Nicolet 5700 spectrometer (Thermo Fisher Scientific Inc., Waltham, MA, USA) equipped with a ZnSe crystal ATR unit and a Bruker Tensor 27 fitted with a SPECAC Golden Gate diamond ATR accessory. Spectra were collected at a resolution of 4 cm^{-1}, averaging 64 scans for each measurement.

2.2.7. Surface Wettability

The contact angles of water and oil on the coatings were evaluated using the sessile drop method with an OCA 15EC contact angle goniometer (DataPhysics Instruments GmbH, Filderstadt, Germany). Measurements were carried out at room temperature (approximately 25 °C) with a precision of ±0.01 mN/m. For each test, droplets of 0.0002 mL were placed on 10 randomly selected spots on the coating surface. The standard deviation of contact angle measurements ranges within 1–2°. Images of the droplets were captured and analyzed using SCA shape analysis software (DataPhysics Instruments GmbH, Germany). Additionally, the surface energy for individual composites was calculated (using the Owens–Wendt method, which involves measuring the contact angle for polar and nonpolar liquids) [32].

2.2.8. SEM

A Hitachi TM-3000 SEM was used to examine the morphology of the pretreated aluminum specimens. The samples of area 10 × 10 mm were graphite coated in order to produce a conductive surface before being placed in the vacuum chamber of the microscope.

3. Results

3.1. Impact Resistance

Due to the high impact strength of the manufactured coatings, the impact rate resulting in mechanical damage in the form of a breakage of the coating structure was taken as the measurement result (Figure 5).

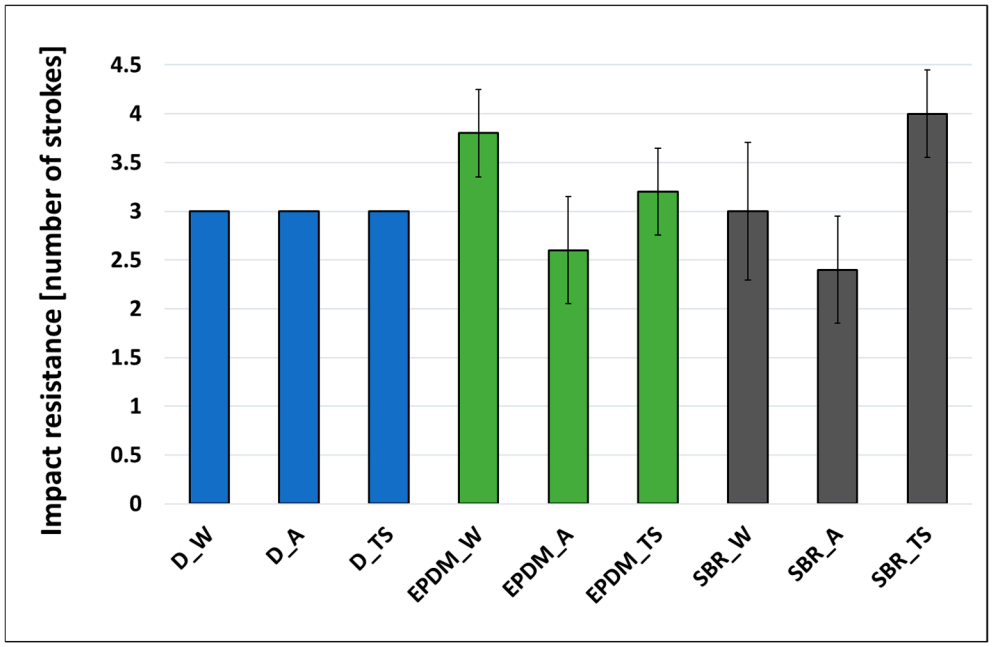

Figure 5. Impact-resistance results of the obtained coatings; D—sample without filler; SBR—sample with SBR filler; EPDM—sample with EPDM filler; W—without aging; A—UV aging; TS—thermal shock.

Firstly, impact tests were carried out on the aluminum substrate alone without the coatings. After the second impact, the aluminum sheet *fractured* (Figure 6).

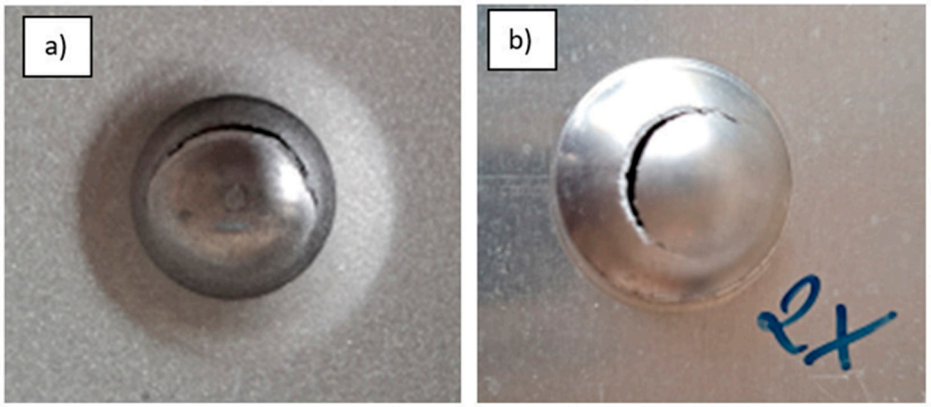

Figure 6. Aluminum substrate after double impact (**a**) front; (**b**) back.

The addition of EPDM fillers improved impact resistance by 25% compared to coatings without fillers. However, the SBR filler in coatings not subjected to ageing processes did not affect the change in impact resistance.

Neither the aging process nor thermal shocks affected the impact resistance of unfilled polyurethane coatings. In each sample, after three impacts, complete rupture of the substrate and coating occurred (Figure 7).

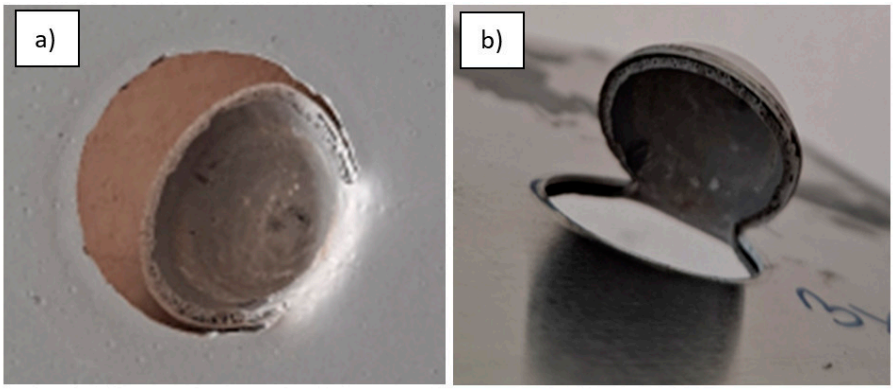

Figure 7. Polyurethane coating without filler after three impact (**a**) front; (**b**) back.

The accelerated aging process in the climate chamber negatively affected the impact resistance. Both EPDM-filled and SBR-filled coatings cracked mostly after two impacts. Similar trends were noticed in the publication [33], which also showed that aging under the influence of UV radiation causes a decrease in the puncture resistance of fabrics impregnated with polyurethane cointaining with fillers. In contrast, the addition of fillers such as SBR and EPDM significantly alters the mechanical behavior of polyurethane coatings, which are subject to thermal shocks. These elastomeric fillers introduce a dual-phase structure, where the flexible rubber domains enhance energy dissipation during impact, thus increasing resistance to mechanical failure. Moreover, they improve crack-bridging ability and provide additional toughness to the coating matrix. As a result, coatings become less brittle and more resistant to sudden stresses, including those induced by thermal expansion or impact.

The highest pull-off strength was observed in coatings with SBR and EPDM fillers subjected to thermal shocks. These coatings showed increased durability under thermal cycling conditions. The coatings with SBR filler were completely destroyed after, on average, the fourth impact.

Furthermore, rubber fillers act as stress concentrators and micro-shock absorbers within the polymer matrix. This leads to improved damping properties and contributes

to the delay in the initiation and propagation of microcracks under dynamic loads. Their compatibility with polyurethane allows good interfacial adhesion, which is crucial for efficient stress transfer and the integrity of the composite structure. Therefore, the incorporation of SBR and EPDM not only enhances mechanical strength but also extends the operational durability of the coatings, especially under fluctuating environmental conditions.

This is consistent with findings in the literature [34], where thermoset epoxy resins reinforced with recycled rubber microparticles demonstrated enhanced mechanical properties. The recycled rubber used as filler was derived from the environmentally responsible disposal of used tires.

3.2. Abrasion Resistance

The abrasion resistance of the obtained polyurethane coatings was evaluated based on the Taber Wear Index (TWI), where higher values indicate greater material loss and thus lower resistance to wear. The test results are presented in Figure 8.

The lowest TWI values, about 1.75, and thus the best abrasion resistance, were observed for unfilled polyurethane coatings (D_W, D_UV, D_ST), with minimal differences between non-aged, UV-aged, and thermally shocked samples. This indicates that pure polyurethane maintains stable wear resistance even under aging conditions, confirming its good durability in long-term use.

In contrast, the introduction of fillers (EPDM and SBR) caused a noticeable increase in TWI (2.18, 3.00, respectively), indicating reduced abrasion resistance. Abrasion resistance is influenced by the type of filler, as well as its content in the material [35,36]. Among the filled samples, coatings with SBR showed the highest wear indices, particularly in the unaged condition (SBR_W), where the average TWI exceeded 3.0. Although UV aging (SBR_UV) and thermal shock (SBR_ST) slightly reduced the value of TWI by 17% and 28%, values remained significantly higher than for unfilled samples.

Coatings modified with EPDM exhibited intermediate wear performance. While EPDM-filled coatings showed increased TWI values (TWI = 2.18), compared to unfilled ones, they maintained better abrasion resistance than their SBR-filled counterparts under all tested conditions. The most abrasion-resistant among the EPDM samples was the thermally shocked coating (TWI = 2.28), suggesting a possible structural tightening or stress-induced stabilization following thermal cycling.

These findings demonstrate that although the addition of rubber fillers (EPDM and SBR) enhances some mechanical properties, such as impact resistance, it simultaneously compromises surface durability under abrasive conditions. The soft, elastomeric nature of these fillers contributes to easier material removal during wear, especially in SBR-modified coatings, which have a lower intrinsic resistance to surface degradation.

Nonetheless, slight improvements in the wear performance of aged, filled coatings suggest that post-processing effects—such as thermal shrinkage or UV-induced crosslinking—may partially mitigate wear mechanisms. However, these effects are insufficient to outperform unfilled polyurethane in terms of abrasion resistance. Similar decreases in abrasion resistance with improvement of other mechanical properties were noted in the publication [37], which reported abrasion tests conducted on a thermoplastic polyurethane resin with ethylene-propylene-diene rubber (EPDM).

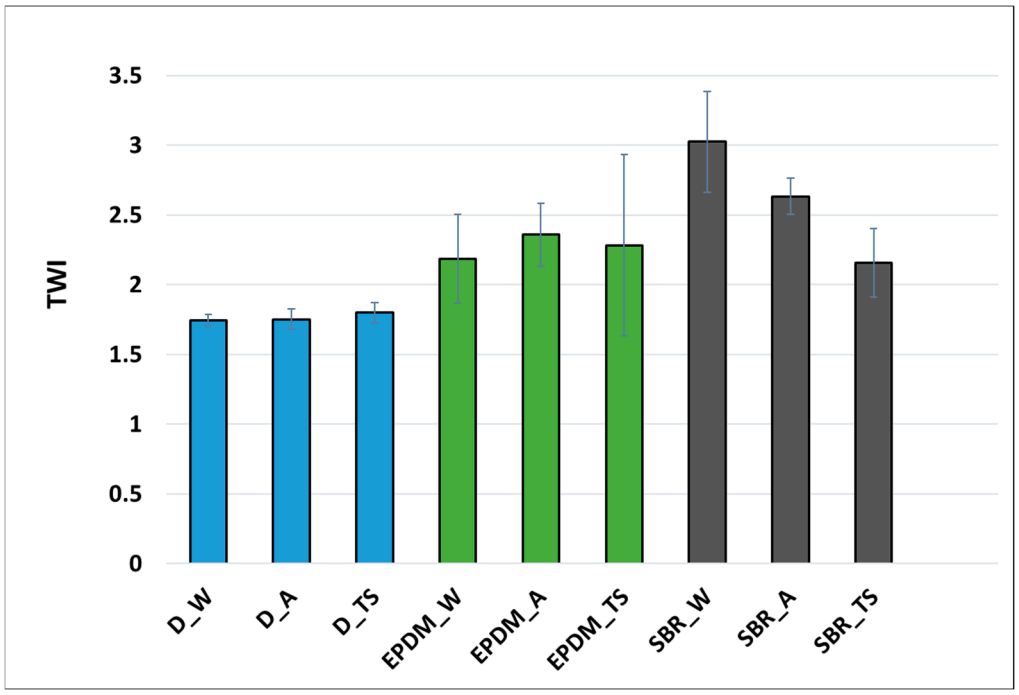

Figure 8. Taber Wear Index of polyurethane coatings with different fillers and aging conditions.

3.3. Thermal Analysis

The differences in the thermal decomposition temperature of the coatings under investigation is prominently illustrated in Figure 9, which presents the TGA (Thermogravimetric Analysis) and DTG (Differential Thermogravimetric) thermograms of the research samples, while Table 2 provides a detailed summary of the key parameters obtained from the evaluation of the TGA/DTG thermograms.

Table 2. Thermal decomposition of the tested materials.

	T_5 [°C]	T_{10} [°C]	R [%]	V_1 [°C]	V_2 [°C]
D_W	268.8	325.8	63.68	375.4	-
EPDM_W	281.0	320.4	64.94	364.9	441.1
SBR_W	282.4	321.2	58.22	384.7	-
D_A	282.9	316.5	48.41	384.3	-
EPDM_A	287.0	324.4	59.18	375.9	441.4
SBR_A	284.8	332.4	62.28	386.2	-
D_TS	280.6	312.4	46.77	385.7	-
EPDM_TS	285.5	321.8	60.89	368.1	441.5
SBR_TS	280.5	328.6	60.82	383.6	-

T_5—the temperature at which the weight loss of the sample reached 5%; T_{10}—the temperature at which the weight loss of the sample reached 10%; R—the residual mass, V_1, V_2—Temperature at which the maximum degradation rate of a given substance occurred.

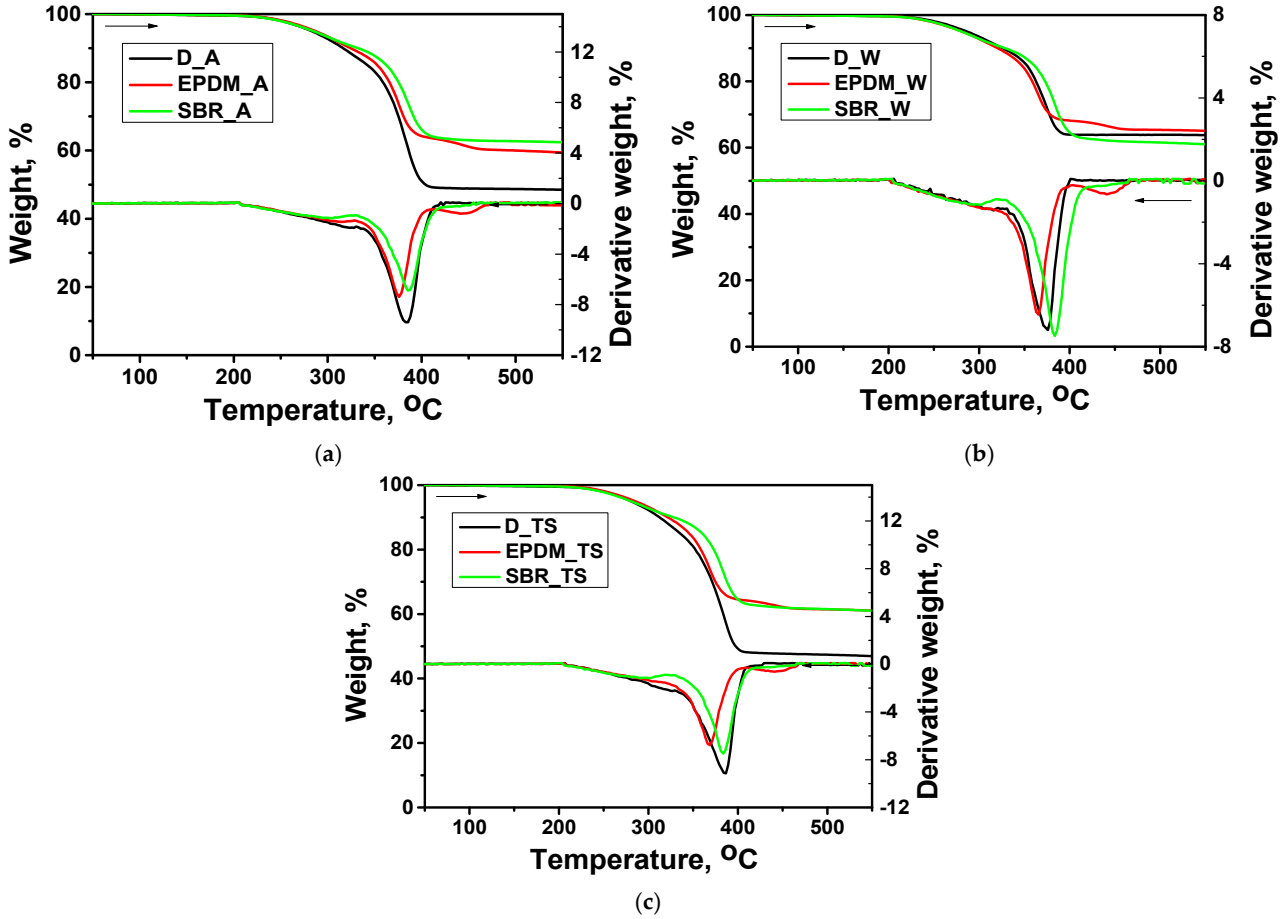

Figure 9. TGA and DTG for the systems: (**a**) without aging; after aging with UV light (**b**); after thermal shock conditions (**c**).

DTG analysis provides a more detailed understanding of the thermal degradation behavior of the tested materials by revealing the rate of mass loss as a function of temperature. Unlike TGA, which indicates the overall weight change, DTG highlights the temperatures at which decomposition occurs most rapidly, allowing for precise identification of degradation stages and their corresponding mechanisms. In this study, DTG data clearly show that the decomposition of the coatings occurs in two distinct stages, consistent with observations reported in the literature [38]. The temperature labeled as V_1 corresponds to the maximum decomposition rate of the hard segments—primarily polyisocyanate components—while V_2 marks the maximum decomposition rate of the soft segments, predominantly composed of polyol moieties [38]. For non-aged polymer coatings, the sample containing SBR rubber waste exhibited the greatest overall mass loss with increasing temperature, whereas the sample with EPDM rubber waste showed the lowest. Notably, both UV aging and thermal shock aging led to significantly reduced mass loss in the rubber-filled samples compared to their non-aged counterparts. All samples initiated thermal degradation at approximately 200 °C. Among non-aged coatings, the SBR-filled sample demonstrated the highest thermal stability, as indicated by the highest decomposition rate occurring at a higher temperature than in other samples. In contrast, the EPDM-filled sample showed the lowest stability, with decomposition peaking at the lowest temperature. This trend persisted across both UV-aged and thermally shocked samples, where SBR-filled coatings consistently outperformed EPDM-filled ones in thermal stability. In the case of thermally shocked samples, the highest thermal stability was observed in both the SBR-filled and unfilled coatings, while the EPDM-filled sample again showed the poorest performance.

TGA revealed a notably high residual mass in the polyurethane samples, exceeding 50% at temperatures above 500 °C in most cases. Given that the exact formulation of the PUR matrix is unknown, the precise origin of this residue remains uncertain. However, such significant thermal stability suggests the presence of components that resist decomposition at elevated temperatures.

3.4. Glass Transition Temperature

The results of the DSC thermal analysis are presented in Figure 10.

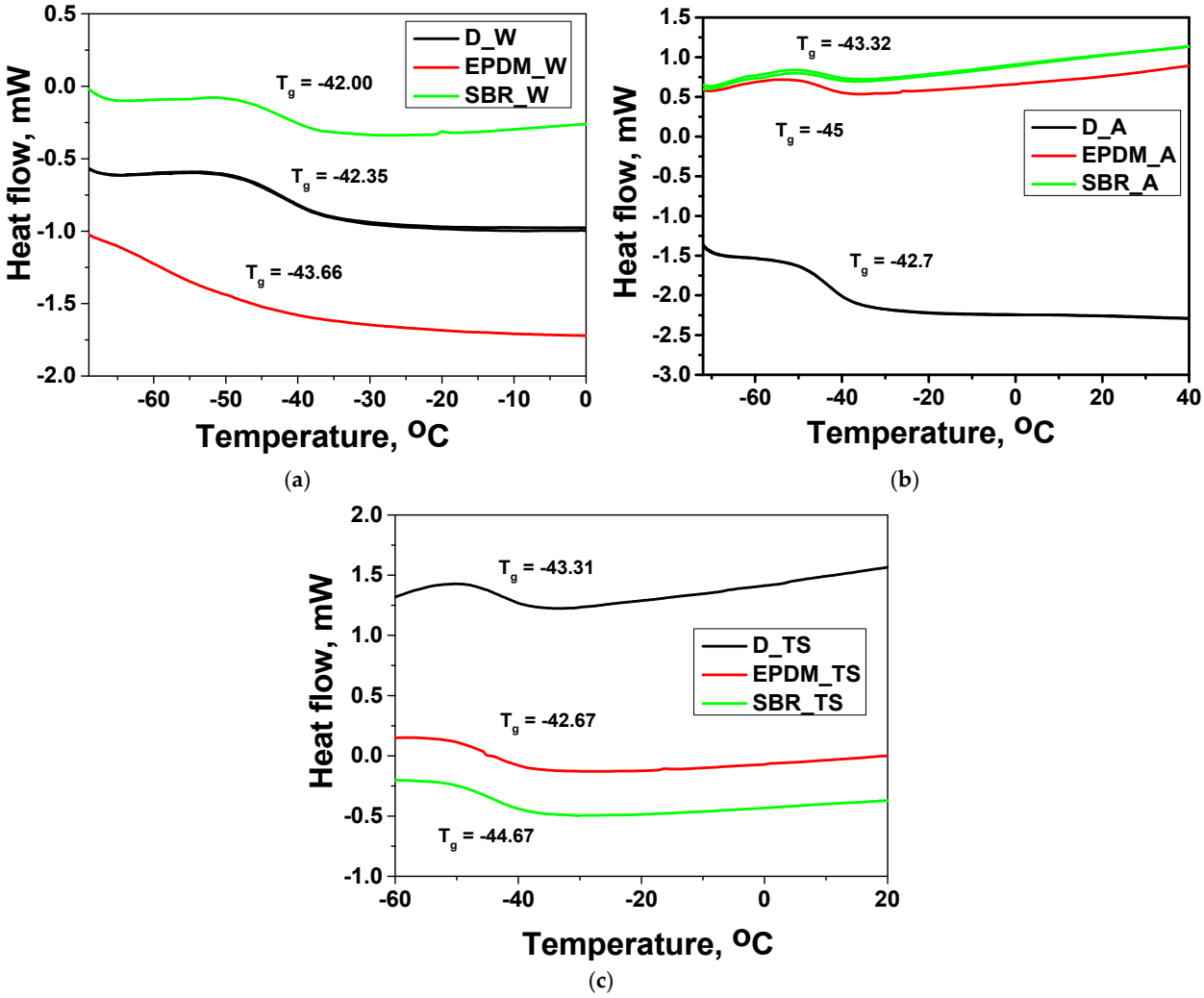

Figure 10. DSC for the systems: (**a**) without aging; after aging with UV light (**b**); after thermal shock conditions (**c**).

The polyurethane matrix exhibits a glass transition temperature (T_g) of −42.35 °C, indicative of the presence of flexible soft segments within the polymer structure, which enhance chain mobility at low temperatures. Exposing the sample to the UV aging process caused this temperature to drop to −42.70 °C, which can be attributed to photo-oxidative degradation leading to increased chain mobility and partial scission of polymer backbones. Conversely, thermal shock aging (D_TS) resulted in a marginal decrease in T_g to −43.31 °C, likely due to restructuring or additional physical crosslinking induced by temperature cycling. A similar trend was observed in the samples containing rubber fillers. In the case of EPDM-filled composites (EPDM_W), the initial T_g was −43.66 °C. After UV aging (EPDM_A), this value dropped significantly to −45 °C, suggesting increased chain flexibility possibly due to photodegradation or chain scission at the filler–

matrix interface. On the other hand, after thermal shock treatment (EPDM_TS), T_g increased to −42.67 °C, implying a more rigid structure potentially caused by filler-induced stabilization or internal stress relaxation. For SBR-filled composites (SBR_W), the initial T_g was −42.00 °C. Interestingly, both UV aging (SBR_A, −43.32 °C) and thermal shock aging (SBR_TS, −44.67 °C) caused further reduction in T_g. This behavior may be related to higher susceptibility of SBR to aging-induced degradation, resulting in more flexible, lower-T_g domains within the matrix.

3.5. FTIR

FTIR analysis was used to assess the changes in the structural changes of the tested polymer coatings, which were subjected to aging processes, as well as to investigate the interactions between the polyurethane matrix and the added rubber waste. Figure 11 shows the FTIR spectra of the tested samples.

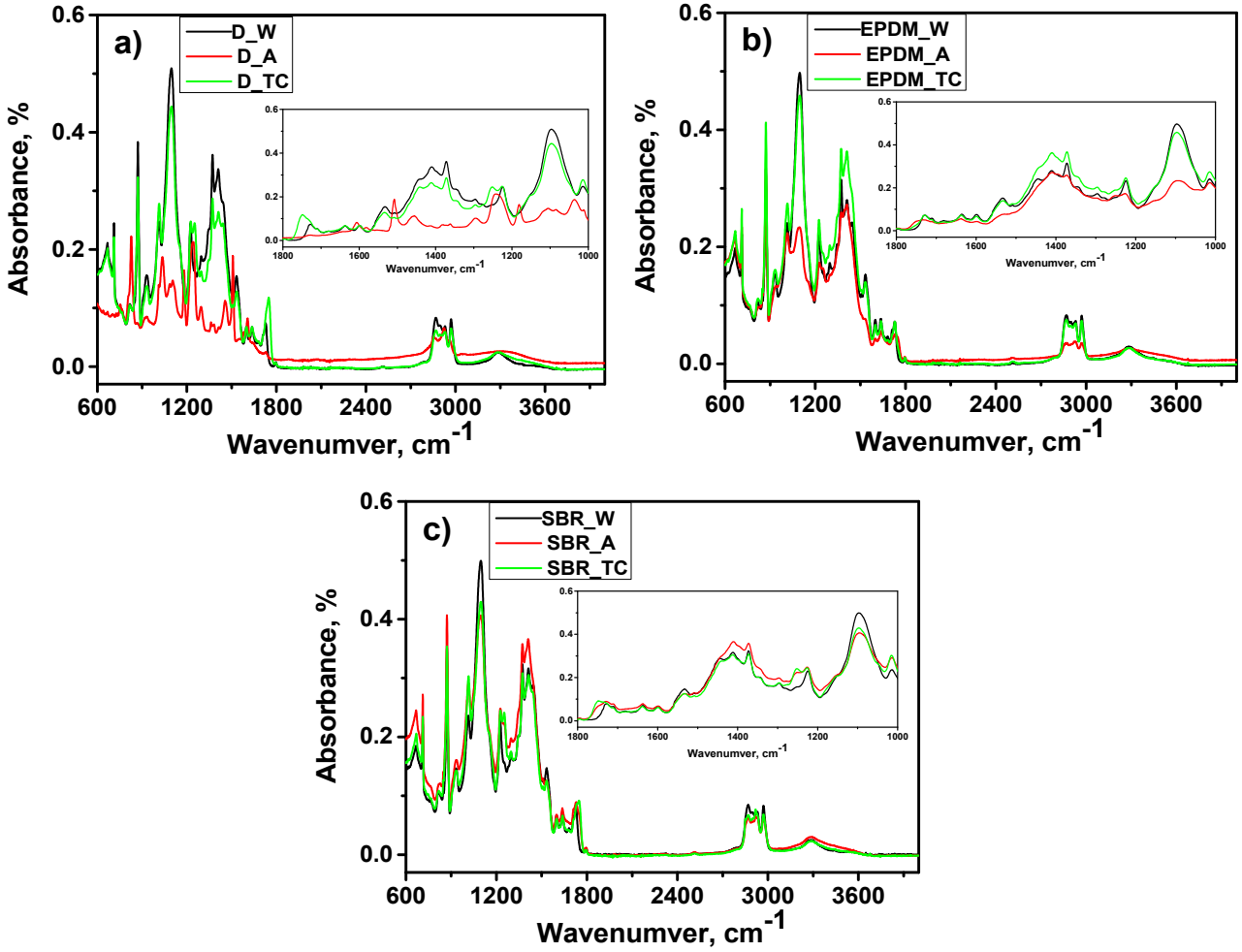

Figure 11. FTIR spectra of polymers: (**a**) D sample; and composite containing: (**b**) EPDM; (**c**) SBR rubber waste.

Polyurethane is a type of polymer composed of repeating urethane linkages (–NHCOO–), typically formed through the reaction between isocyanates and polyols. In the spectra shown in Figure 11, the same characteristic bands can be observed in all tested samples. Absorption bands observed near 3350 cm^{-1} correspond to the stretching vibrations of N–H bonds, while the bands in the 1650–1580 cm^{-1} range are attributed to N–H bending vibrations, both characteristic of urethane groups [39]. Bands observed between 2840 and 2960 cm^{-1} correspond to the symmetric and asymmetric stretching

vibrations of C–H bonds in –CH_2– groups, while those between approximately 1550 and 1375 cm^{-1} are attributed to the bending vibrations of these bonds. The band at 1218 cm^{-1} corresponds to the stretching vibration of C(O)O–C groups [40]. The absorption band around 1100 cm^{-1} is typically associated with C–O–C stretching vibrations (ether bonds) or C–O bonds in soft segments derived from polyols. It can also partially overlap with C–N vibrations.

The absence of absorption bands near 2280 cm^{-1}, which would originate from the stretching vibrations of the –N=C=O (isocyanate) group, indicates the complete consumption of isocyanate groups, confirming a complete polyaddition reaction [39,41,42]. Absorption bands at the wave number of ~1730 cm^{-1} are associated with the carbonyl group [43]. The literature reports the existence of two distinct contributions in certain polyurethane systems, related to carbonyl groups involved in weak and strong hydrogen bonding. The first contribution is associated with disordered, localized urethane groups, with IR absorption bands appearing between 1722 and 1700 cm^{-1}. The second corresponds to locally ordered urethane groups, exhibiting bands in the range of 1711 to 1684 cm^{-1} [39].

In polyurethanes, aging under UV light irradiation results in the disappearance or significant reduction of carbonyl bands. This occurs because UV radiation induces photodegradation processes that break down carbonyl-containing groups, such as urethane and ester linkages, leading to chain scission and the formation of smaller, less conjugated fragments [41,44]. These fragments absorb less strongly in the carbonyl region. Moreover, UV exposure can trigger oxidation reactions that convert carbonyl groups into other species, thereby reducing their characteristic FTIR absorbance. The progressive hydrolysis of the polyol segment in the polyurethane, particularly the ester linkages, is evidenced by the reduction also in the intensity of characteristic absorption bands at 1120 cm^{-1} and 1078 cm^{-1} (Figure 11a). This process is further supported by the emergence of new bands at 1682 cm^{-1}, 1273 cm^{-1}, 1189 cm^{-1}, 916 cm^{-1}, and 733 cm^{-1}. These bands indicate the formation of such as adipic acid, a characteristic degradation product of PUR [44].

Thermal shock aging in polyurethanes leads to the weakening of carbonyl bonds and causes a shift of the C=O absorption bands toward longer wavenumbers. This shift may indicate the formation of new, more complex oxygen-containing structures or changes in the chemical environment around the carbonyl groups, affecting their characteristic vibrations (corresponding to carbonyls, e.g., ketones, aldehydes, peroxides) [45,46].

The effect of aging on the tested polymer coatings containing EPDM or SBR rubber waste is smaller than in the case of samples without added fillers. A new band in the range of 1730 cm^{-1} – 1750 cm^{-1} appeared, which may indicate the formation of new peroxide structures resulting from oxidation or the formation of new carbonyl bonds, i.e., quinone-imide structures [46]. This is especially visible in the case of samples treated under thermal shock conditions.

Polyurethane coatings containing EPDM exhibited greater resistance to UV-induced degradation compared to those modified with SBR or without any filler. This enhanced stability can be attributed to the saturated, non-polar structure of EPDM, which lacks readily oxidizable sites such as double bonds or aromatic groups, making it inherently more resistant to photooxidative processes. In contrast, SBR—containing unsaturated butadiene segments—is more prone to UV-induced chain scission and oxidation, which contributes to more noticeable changes in the material.

3.6. Contact Angle

To investigate the contact angle and determine the surface free energy, water and oil were used as test liquids. The Contact Angle System OCA goniometer from Dataphysics was used for the measurements. The table presents the obtained microscopic images and

contact angle values for PUR polymer coatings, PUR containing EPDM and SBR rubber waste, not subjected to aging processes (Table 3). Analogously, the results are presented for the tested polymer coatings that were subjected to UV light aging processes and aging under thermal shock conditions.

Table 3. Hydrophilic-hydrophobic properties of coatings, images, and values of water contact angle Θ and surface energy (SE).

Sample	**D_W**	**EPDM_W**	**SBR_W**
Wetting angle image	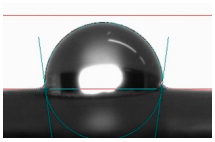	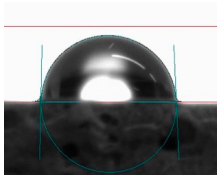	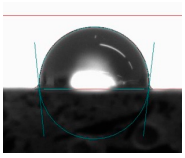
Contact angle, Θ	97.4°	87.5°	96.5°
SE [mN/m]	80	65	79
Sample	D_A	EPDM_A	SBR_A
Wetting angle image	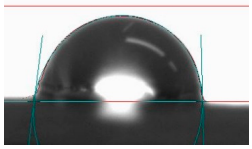	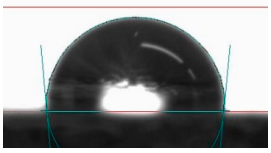	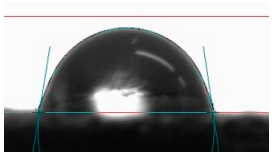
Contact angle, Θ	88.7°	95.2°	82°
SE [mN/m]	69	86	58
Sample	D_TS	EPDM_TS	SBR_TS
Wetting angle image	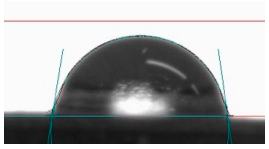	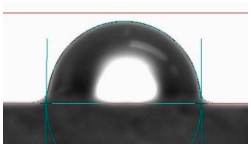	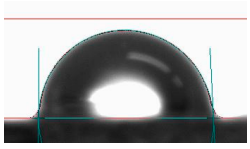
Contact angle, Θ	82°	89.7°	89°
SE [mN/m]	50	67	78

Analyzing the results for the tested polymer coatings not subjected to the aging process (Table 3), it can be seen that the reference PUR sample showed the highest contact angle value of Θ = 97.4° (SE = 80 mN/m), indicating poor wettability, i.e., a hydrophobic surface. The addition of SBR rubber waste to the polymer coating caused the wetting angle value slight decrease to Θ = 96.5° (SE = 79 mN/m). The coating containing EPDM rubber waste had the lowest wetting angle value, reaching Θ = 87.5°, and the lowest SE value (65 mN/m). This trend demonstrates that both SBR and EPDM waste additives reduce the surface hydrophobicity of the coatings, but EPDM to a greater extent. This can be explained by the modification of surface polarity, rubber particles, especially EPDM, may introduce microscopic surface roughness and more polar functional groups, thus improving water adhesion and leading to a decrease in Θ.

In the case of coatings subjected to UV light aging, the highest wetting angle value was achieved by the sample with the addition of EPDM rubber waste, reaching Θ = 95.2°. The sample without the addition of rubber waste showed the value of the wetting angle (Θ = 88.7°), while the lowest wetting angle was observed for the sample with the addition of SBR rubber waste with the value of Θ = 82°. The observed differences can be attributed to the photo-oxidative degradation mechanisms induced by UV exposure. In samples without rubber filler or with SBR, UV light likely caused oxidation of the polymer surface and the formation of polar oxygen-containing groups (such as carbonyl or hydroxyl), which significantly increased surface energy and wettability. In contrast, EPDM-modified

coatings were more resistant to UV-induced oxidation, likely due to EPDM's saturated backbone and stabilizing effects, which maintained a higher contact angle and thus greater hydrophobicity.

The results obtained from coatings subjected to thermal shock aging (D_TS, SBR_TS, EPDM_TS) confirm similar trends. Thermal treatment often leads to oxidation of the polymer surface, introducing polar functional groups such as hydroxyl (-OH), carbonyl (C=O), or carboxyl (-COOH) groups. These groups significantly increase hydrophilicity of the SBR surface. The formation of additional groups, specifically C=O carbonyl groups, can be observed on the FTIR spectrum, suggesting that new carbonyl groups are being formed as a result of degradation processes like oxidation or the formation of new bonds during the aging process. For the EPDM-containing sample (EPDM_TS), an increase in the contact angle was observed ($\Theta = 89.7°$), indicating enhanced hydrophobicity compared to its unaged counterpart. This effect may be linked to surface restructuring or orientation of non-polar EPDM segments at the interface during thermal cycling.

4. Conclusions

In this work, polyurethane coatings, both unfilled and filled with waste rubber (SBR and EPDM), were tested, which were subjected to the aging process in a climatic chamber and thermal shocks. Based on the obtained results, the following conclusions can be drawn:

1. Impact and Abrasion Resistance
   Polyurethane coatings without fillers maintained their impact and abrasion resistance after both UV ageing and thermal shock exposure.
   The addition of EPDM and SBR rubber fillers:
   - Improved impact resistance under thermal shock conditions.
   - Reduced abrasion resistance by about 40%, especially with SBR particles, which accelerated wear with surface material loss of about 25% in the case of EPDM filler.

   The ageing process had a negative impact on impact resistance. Coatings with EPDM filler were characterized by a lower impact resistance by 20%, and those with SBR filler by 30%.
2. Chemical Structure and Degradation
   FTIR spectroscopy confirmed the presence of characteristic polyurethane functional groups across all samples. PUR coatings are significantly degraded by UV light. Fillers, especially EPDM contributed to chemical stabilization, slowing down UV-induced degradation. Thermal shocks led to formation of new groups on the surface containing oxygen and rearrangement of hydrogen bonds.
3. Hydrophobicity and Surface Properties
   The addition of rubber waste reduced the contact angle, indicating lower surface hydrophobicity. EPDM demonstrated better oxidation resistance and retained higher hydrophobicity after thermal shock compared to SBR.
4. Thermal properties
   Ageing processes (UV and thermal shock) led to a decrease in T_g for SBR-containing coatings. This made the material more flexible but also more prone to degradation.
   The SBR-filled coatings exhibited higher thermal stability, decomposing at higher temperatures. EPDM-filled coatings showed lower thermal stability, decomposing at more rapidly.

Author Contributions: Conceptualization, P.M.-T.; methodology, P.M.-T., M.R; validation, P.M.-T., M.F.; formal analysis, P.M.-T. and M.R; investigation, M.R, P.M.-T., S.P.,; resources, P.M.-T., M.R.;

writing—original draft preparation, M.R and P.M.-T.; writing—review and editing, M.R. P.M.-T.; project administration, P.M.-T.; funding acquisition, P.M.-T. All authors have read and agreed to the published version of the manuscript.

Funding: This research received no external funding.

Institutional Review Board Statement: Not applicable.

Informed Consent Statement: Not applicable

Data Availability Statement: Data are contained within the article.

Acknowledgments: Work carried out as part of a research internship KMM-VIN Research Fellowship. The part of this work was supported by the Polish Ministry of Education and Science.

Conflicts of Interest: The authors declare no conflict of interes.

Abbreviations

D_W	sample without filler and without aging
SBR_W	sample with SBR filler and without aging
EPDM_W	sample with EPDM filler and without aging
D_A	sample without filler after UV aging
SBR_A	sample with SBR filler after UV aging
EPDM_A	sample with EPDM filler after UV aging
D_TS	sample without filler after thermal shock
SBR_TS	sample with SBR filler after thermal shock
EPDM_TS	sample with EPDM filler after thermal shock

References

1. Alfayez, S.A.; Suleiman, A.R.; Nehdi, M.L. Recycling Tire Rubber in Asphalt Pavements: State of the Art. *Sustainability* **2020**, *12*, 9076. https://doi.org/10.3390/su12219076.
2. Hashamfirooz, M.; Dehghani, M.H.; Khanizadeh, M.; Aghaei, M.; Bashardoost, P.; Hassanvand, M.S.; Hassanabadi, M.; Momeniha, F. A systematic review of the environmental and health effects of waste tires recycling. *Heliyon* **2025**, *11*, e41909. https://doi.org/10.1016/j.heliyon.2025.e41909.
3. Moreno, T.; Balasch, A.; Bartrolí, R.; Eljarrat, E. A new look at rubber recycling and recreational surfaces: The inorganic and OPE chemistry of vulcanised elastomers used in playgrounds and sports facilities. *Sci. Total Environ.* **2023**, *868*, 161648. https://doi.org/10.1016/j.scitotenv.2023.161648.
4. Nuzaimah, M.; Sapuan, S.M.; Nadlene, R.; Jawaid, M. Recycling of waste rubber as fillers: A review. *IOP Conf. Ser. Mater. Sci. Eng.* **2018**, *368*, 12016. https://doi.org/10.1088/1757-899X/368/1/012016.
5. Hejna, A.; Korol, J.; Przybysz-Romatowska, M.; Zedler, Ł.; Chmielnicki, B.; Formela, K. Waste tire rubber as low-cost and environmentally-friendly modifier in thermoset polymers—A review. *Waste Manag.* **2020**, *108*, 106–118. https://doi.org/10.1016/j.wasman.2020.04.032.
6. Vermette, P.; Griesser, H.J.; Laroche, G.; Guidoin. *Biomedical Applications of Polyurethanes*: *Tissue Engineering Intelligence Unit 6*; Landes Bioscience: Georgetown, TX, USA, 2001; ISBN 1-58706-023-X.
7. Chattopadhyay, D.K.; Raju, K. Structural engineering of polyurethane coatings for high performance applications. *Prog. Polym. Sci.* **2007**, *32*, 352–418. https://doi.org/10.1016/j.progpolymsci.2006.05.003.
8. Golling, F.E.; Pires, R.; Hecking, A.; Weikard, J.; Richter, F.; Danielmeier, K.; Dijkstra, D. Polyurethanes for coatings and adhesives–chemistry and applications. *Polym. Int.* **2019**, *68*, 848–855. https://doi.org/10.1002/pi.5665.
9. Xie, F.; Zhang, T.; Bryant, P.; Kurusingal, V.; Colwell, J.M.; Laycock, B. Degradation and stabilization of polyurethane elastomers. *Prog. Polym. Sci.* **2019**, *90*, 211–268. https://doi.org/10.1016/j.progpolymsci.2018.12.003.
10. Pęczek, E.; Pamuła, R.; Białowiec, A. Recycled Waste as Polyurethane Additives or Fillers: Mini-Review. *Materials* **2024**, *17*, 1013. https://doi.org/10.3390/ma17051013.
11. Das, A.; Mahanwar, P. A brief discussion on advances in polyurethane applications. *Adv. Ind. Eng. Polym. Res.* **2020**, *3*, 93–101. https://doi.org/10.1016/j.aiepr.2020.07.002.

12. Therias, S.; Rapp, G.; Masson, C.; Gardette, J.-L. Limits of UV-light acceleration on the photooxidation of low-density polyethylene. *Polym. Degrad. Stab.* **2021**, *183*, 109443. https://doi.org/10.1016/j.polymdegradstab.2020.109443.
13. Xu, X.; Deng, J.; Nie, S.; Lan, Z.; Xu, Z. Effect of Thermal Aging on Mechanical Properties and Morphology of GF/PBT Composites. *Polymers* **2023**, *15*, 3798. https://doi.org/10.3390/polym15183798.
14. Wang, J.; Gu, Z.; Zhao, J.; Zhang, S.; Li, P.; Meng, C.; Sui, J.; Zhang, X.; Hu, S.; Pan, J.; et al. Aging behavior of three-proof polyurethane coatings under UV radiation. *Polimery* **2022**, *67*, 433–437. https://doi.org/10.14314/polimery.2022.9.4.
15. Mayer, P.; Lubecki, M.; Stosiak, M.; Robakowska, M. Effects of surface preparation on the adhesion of UV-aged polyurethane coatings. *Int. J. Adhes. Adhes.* **2022**, *117*, 103183. https://doi.org/10.1016/j.ijadhadh.2022.103183.
16. Ishida, T.; Kitagaki, R. Mathematical Modeling of Outdoor Natural Weathering of Polycarbonate: Regional Characteristics of Degradation Behaviors. *Polymers* **2021**, *13*, 820. https://doi.org/10.3390/polym13050820.
17. Wang, X.; Andriani, Y.; Lim, P.C.; Lee, C.J.J.; Liu, S.; Lau, B.L.; Zhang, X. Effect of Thermal Cycling on the Thermal and Mechanical Properties of Dielectric Materials. *IEEE Trans. Compon. Packag. Manufact. Technol.* **2020**, *10*, 1166–1174. https://doi.org/10.1109/TCPMT.2020.2998492.
18. Pintus, V.; Wei, S.; Schreiner, M. Accelerated UV ageing studies of acrylic, alkyd, and polyvinyl acetate paints: Influence of inorganic pigments. *Microchem. J.* **2016**, *124*, 949–961. https://doi.org/10.1016/j.microc.2015.07.009.
19. Bhargava, S.; Kubota, M.; Lewis, R.D.; Advani, S.G.; Prasad, A.K.; Deitzel, J.M. Ultraviolet, water, and thermal aging studies of a waterborne polyurethane elastomer-based high reflectivity coating. *Prog. Org. Coat.* **2015**, *79*, 75–82. https://doi.org/10.1016/j.porgcoat.2014.11.005.
20. Bartolomeo, P.; Irigoyen, M.; Aragon, E.; Frizzi, M.A.; Perrin, F.X. Dynamic mechanical analysis and Vickers micro hardness correlation for polymer coating UV ageing characterisation. *Polym. Degrad. Stab.* **2001**, *72*, 63–68. https://doi.org/10.1016/S0141-3910(00)00203-2.
21. Frigione, M.; Rodríguez-Prieto, A. Can Accelerated Aging Procedures Predict the Long Term Behavior of Polymers Exposed to Different Environments? *Polymers* **2021**, *13*, 2688. https://doi.org/10.3390/polym13162688.
22. Qin, J.; Jiang, J.; Tao, Y.; Zhao, S.; Zeng, W.; Shi, Y.; Lu, T.; Guo, L.; Wang, S.; Zhang, X.; et al. Sunlight tracking and concentrating accelerated weathering test applied in weatherability evaluation and service life prediction of polymeric materials: A review. *Polym. Test.* **2021**, *93*, 106940. https://doi.org/10.1016/j.polymertesting.2020.106940.
23. Xiong, G.; Al-Deen, S.; Guan, X.; Qin, Q.; Zhang, C. Economic and Environmental Benefit Analysis between Crumb Rubber Concrete and Ordinary Portland Cement Concrete. *Sustainability* **2024**, *16*, 4758. https://doi.org/10.3390/su16114758.
24. Zhou, M.; Liu, J.; Hou, G.; Yang, H.; Zhang, L. Study on structures, dynamics and mechanical properties of styrene butadiene rubber (SBR)/silica interfaces: A fully atomistic molecular dynamics. *Polymer* **2021**, *218*, 123523. https://doi.org/10.1016/j.polymer.2021.123523.
25. Tayefi, M.; Eesaee, M.; Hassanipour, M.; Elkoun, S.; David, E.; Nguyen-Tri, P. Recent progress in the accelerated aging and lifetime prediction of elastomers: A review. *Polym. Degrad. Stab.* **2023**, *214*, 110379. https://doi.org/10.1016/j.polymdegradstab.2023.110379.
26. *PN-EN ISO 2808:2008*; Paints and Varnishes-Coating Thickness Determination. ISO: Warsaw, Poland, 2008.
27. Guha, R.D.; Danilov, E.O.; Berkowitz, K.; Oluwajire, O.; Grace, L.R. Consequences of Humidity Cycling on the Moisture Absorption Characteristics of Epoxy Resins with Different Network Architectures. *ACS Appl. Polym. Mater.* **2023**, *5*, 400–411. https://doi.org/10.1021/acsapm.2c01570.
28. Segerström, S.; Ruyter, I.E. Effect of thermal cycling on flexural properties of carbon-graphite fiber-reinforced polymers. *Dent. Mater.* **2009**, *25*, 845–851. https://doi.org/10.1016/j.dental.2008.12.007.
29. *ISO 4892-1:2016*; Methods of Exposure to Laboratory Light Sources, Part 1 and Part 2 The SUNTEST, Plastics. ISO: Warsaw, Poland, 2016.
30. *EN ISO 6272-1:2011*; Paints and Varnishes-Rapid-Deformation (Impact Resistance) Tests—Part 1: Falling-Weight Test, Large-Area Indenter. ISO: Geneva, Switzerland, 2011.
31. *ASTM D4060-10*; Standard Test Method for Abrasion Resistance of Organic Coatings by the Taber Abraser. ASTM International: West Conshohocken, PA, USA, 2015.
32. Rudawska, A.; Jacniacka, E. Analysis for determining surface free energy uncertainty by the Owen–Wendt method. *Int. J. Adhes. Adhes.* **2009**, *29*, 451–457. https://doi.org/10.1016/j.ijadhadh.2008.09.008.
33. Acierno, D.; Graziosi, L.; Patti, A. Puncture Resistance and UV aging of Nanoparticle-Loaded Waterborne Polyurethane-Coated Polyester Textiles. *Materials* **2023**, *16*, 6844. https://doi.org/10.3390/ma16216844.
34. Valášek, P.; Žarnovský, J.; Müller, M. Thermoset Composite on Basis of Recycled Rubber. *Adv. Mater. Res.* **2013**, *801*, 67–73.

35. Wiewióra, M.; Żaba, K.; Kuczek, Ł.; Balcerzak, M.; Madej, M. Analysis of Wear Resistance of Metallic-Reinforced Polyurethane Resin Composites for Sheet Metal Forming. *Adv. Mater. Sci.* **2024**, *24*, 18–29. https://doi.org/10.2478/adms-2024-0015.
36. Nassar, A.; Younis, M.; Ismail, M.; Nassar, E. Improved Wear-Resistant Performance of Epoxy Resin Composites Using Ceramic Particles. *Polymers* **2022**, *14*, 333. https://doi.org/10.3390/polym14020333.
37. Tan, J.; Mei Ding, Y.; Tao He, X.; Liu, Y.; An, Y.; Min Yang, W. Abrasion resistance of thermoplastic polyurethane materials blended with ethylene–propylene–diene monomer rubber. *J Appl. Polym. Sci* **2008**, *110*, 1851–1857. https://doi.org/10.1002/app.28756.
38. Wolska, A.; Goździkiewicz, M.; Ryszkowska, J. Thermal and mechanical behaviour of flexible polyurethane foams modified with graphite and phosphorous fillers. *J. Mater. Sci.* **2012**, *47*, 5627–5634. https://doi.org/10.1007/s10853-012-6433-z.
39. Zimmer, B.; Nies, C.; Schmitt, C.; Possart, W. Chemistry, polymer dynamics and mechanical properties of a two-part polyurethane elastomer during and after crosslinking. Part I: Dry conditions. *Polymer* **2017**, *115*, 77–95. https://doi.org/10.1016/j.polymer.2017.03.020.
40. Barszczewska-Rybarek, I.; Jaszcz, K.; Chladek, G.; Grabowska, P.; Okseniuk, A.; Szpot, M.; Zawadzka, M.; Sokołowska, A.; Tarkiewicz, A. Characterization of changes in structural, physicochemical and mechanical properties of rigid polyurethane building insulation after thermal aging in air and seawater. *Polym. Bull.* **2022**, *79*, 3061–3083. https://doi.org/10.1007/s00289-021-03632-x.
41. Mayer-Trzaskowska, P.; Robakowska, M.; Gierz, Ł.; Pach, J.; Mazur, E. Observation of the Effect of Aging on the Structural Changes of Polyurethane/Polyurea Coatings. *Polymers* **2023**, *16*, 23. https://doi.org/10.3390/polym16010023.
42. Beneš, H.; Černá, R.; Ďuračková, A.; Látalová, P. Utilization of Natural Oils for Decomposition of Polyurethanes. *J. Polym. Environ.* **2012**, *20*, 175–185. https://doi.org/10.1007/s10924-011-0339-8.
43. Murali, A.; Gurusamy-Thangavelu, S.A.; Jaisankar, S.N.; Mandal, A.B. Enhancement of the physicochemical properties of polyurethane–perovskite nanocomposites via addition of nickel titanate nanoparticles. *RSC Adv.* **2015**, *5*, 102488–102494. https://doi.org/10.1039/C5RA17922J.
44. Zhang, X.; Yin, Z.; Xiang, S.; Yan, H.; Tian, H. Degradation of Polymer Materials in the Environment and Its Impact on the Health of Experimental Animals: A Review. *Polymers* **2024**, *16*, 2807. https://doi.org/10.3390/polym16192807.
45. Chudzik, J.; Bieliński, D.M.; Bratychak, M.; Demchuk, Y.; Astakhova, O.; Jędrzejczyk, M.; Celichowski, G. Influence of Modified Epoxy Resins on Peroxide Curing, Mechanical Properties and Adhesion of SBR, NBR and XNBR to Silver Wires. Part I: Application of Monoperoxy Derivative of Epoxy Resin (PO). *Materials* **2021**, *14*, 1320. https://doi.org/10.3390/ma14051320.
46. Yousif, E.; Haddad, R. Photodegradation and photostabilization of polymers, especially polystyrene: Review. *Springerplus* **2013**, *2*, 398. https://doi.org/10.1186/2193-1801-2-398.